Sound & Vibration 2026, 60(6), 4383.
https://doi.org/10.59400/sv4383

Article

Effect of fillet radius on nonlinear damping identification in spur gear systems: application of Sparse Identification of Nonlinear Dynamics (SINDy)

Nourhaine Yousfi*, Rania Maktouf, Ali Akrout, Lassaad Walha, Mohamed Haddar

Mechanics, Modelling and Production Research Laboratory (LA2MP), Engineering National School of Sfax, University of Sfax, Tunisia
*** Corresponding author:** Nourhaine Yousfi, Email: nourhaineali454@gmail.com

CITATION

Yousfi N, Maktouf R, Akrout A, et al. Effect of fillet radius on nonlinear damping identification in spur gear systems: application of Sparse Identification of Nonlinear Dynamics (SINDy). Sound & Vibration. 2026; 60(6): 4383.
https://doi.org/10.59400/sv4383

COPYRIGHT

Copyright © 2026 by author(s). *Sound & Vibration* is published by Academic Publishing Pte Ltd. This work is licensed under the Creative Commons Attribution (CC BY) license.
https://creativecommons.org/licenses/by/4.0/

Abstract: Sparse Identification Approach of nonlinear dynamics (SINDy) is gaining significant interest due to their ability to identify nonlinear damping with only input data. However, its application to nonlinear mechanical systems with time-varying stiffness has not been widely explored. Here, we prove the SINDY method to include time varying stiffness conditions. In numerical models used for the development and validation of such method, fillet radius is often neglected. The present article addresses this knowledge gap by investigating the effects of fillet radius on the efficacy of SINDy, with modified library to include time varying stiffness effect, in identifying the nonlinear damping model in spur gears systems. A numerical modeling and parametric approach, is adopted to evaluate the effect of the fillet radius (R_f) on the nonlinear identification process. Three distinct modeling scenarios are considered where the fillet radius directly affects the time-varying mesh stiffness, the fillet radius influences the nonlinear contact law, and the effect of fillet radius is modeled as a geometric offset in the contact deformation. This multi-scenario framework allows a comprehensive assessment of how geometric variations influence both the system dynamics and the identified nonlinear parameters within the SINDY framework. The impacts of considering fillet radius on the nonlinear damping coefficients identification process are investigated. This work is the first to explicitly investigate the impact of fillet radius on nonlinear damping identification using an extended SINDy framework with time-varying stiffness. The results prove that SINDy approach is directly influenced by geometric modifications.

Keywords: damping identification approach; gears systems; SINDy; fillet radius; time-varying stiffness

1. Introduction

Nonlinear dynamics in gear systems have received considerable research attention. Nonlinearity in gear transmission is mainly due to a variety of factors, which include time-varying mesh stiffness, backlash, and geometric deviations, such as changes in the fillet radius [1,2]. In addition, accurately modeling and identifying damping in nonlinear dynamic systems remains a significant challenge [3,4]. The recent research works have shown increasing attention paid to developing the parameterized identification methods, which allow one to separate the contribution of both linear and nonlinear damping. For example, Al-Hababi et al. [5] conducted an extensive analysis of approaches applied to identify nonlinear damping, where the benefits and drawbacks of such methods were described in detail. According to the results obtained by the authors, the use of nonlinear damping allows one to create a more precise and realistic dynamic model in comparison with the linear ones. In this regard, Nourhaine et al. [6] proposed a novel method for identifying nonlinear damping under noisy conditions using a combination of Continuous Wavelet Transform (CWT) and Long Short-Term Memory (LSTM). Damping identification

includes a variety of algorithms used from input data, such as Sparse Identification of Nonlinear Dynamics (SINDy) [7-9]. Specifically, the SINDy is the method of modeling nonlinear parameters using input data, consisting of the minimum set of necessary terms, through sparse regression [10]. Therefore, it is worth highlighting some benefits of the SINDy framework, such as high accuracy in cases of small sample sizes [11], possibility to work with strongly nonlinearity problems [12], and its robustness in the presence of noise [13]. Compared to LSTM and state-based methods, SINDy offers key advantages for damping identification, including explicit and interpretable governing equations, direct estimation of physical damping coefficients, and the ability to capture nonlinear effects by incorporating physics-informed basis functions into the function library [14,15]. Moreover, it requires relatively limited data and allows the incorporation of prior physical knowledge, making it an efficient and reliable approach for nonlinear dynamical systems [16,17]. Recent findings in the field of structural dynamics have shown the significance of using numerical analysis and modeling techniques for nonlinear structures under dynamic loadings [18,19]. It was found that dynamic responses were highly sensitive to structural properties and there was a necessity for reliable methods of modeling and identification of the behavior in cases of nonlinear and time-dependent response of such systems. Thus, one of the motivations of employing physics-based machine learning techniques is parameter identification in nonlinear systems. The SINDy method has subsequently been generalized to address a broad variety of applications for nonlinear systems. Adam Purnomo et al. [20] proposed a generalized form of Lagrangian-SINDy to reconstruct the Lagrangian of dynamical systems from noisy observations. The robustness of the approach was evaluated under different noise conditions using four distinct mechanical systems. J.-Ch. Loiseau et al. [21] presented an extended SINDy framework by integrating physical constraints into the regression procedure, particularly for quadratic nonlinearities, and is evaluated on two distinct flow configurations. [22] proposed a framework that employs the SINDy model in the data-driven approach for modeling the air path of a diesel engine with a nonlinear model predictive control (NMPC) strategy under system constraints. In addition to mechanical systems, SINDy-based approaches have been widely utilized in fields such as fluid mechanics, physical sciences [23], and biological systems [24] to model the dynamic behaviors. SINDy was extended to deal with non-autonomous systems via time dependence or forcing within the function library, thus allowing for the discovery of systems with time-varying coefficients [25]. However, its application to nonlinear mechanical systems with specific harmonic representation of stiffness has not been widely explored. This study aims to overcome these limits by implementing a time-varying stiffness model using Fourier series into the SINDy formulation. In this work, the classical SINDy framework is extended to account for time-varying system parameters. In particular, the stiffness is modeled as a time-dependent function K(t), expressed using a Fourier series. This time-varying parameter is incorporated into the library of candidate functions, allowing the identification of governing equations that explicitly depend on both the system states and the varying stiffness. The contribution of this work goes beyond the incorporation of time-varying stiffness, as it also provides a systematic study of the effect of the radius fillet Rf on the identification process, highlighting its role in the accuracy and robustness of the resulting model. several studies have examined the effect of the radius fillet Rf to enhance the operational efficiency and performance of gears. For example, Abderrahim et al. [26] presented the effect of the fillet radius on the gear mesh stiffness. The influence of several fillet configuration parameters is evaluated via stress distribution analysis [27].

S. Senthilvelan et al. [28] presented the effect of fillet size on the gear system stress using finite element method (FEM). Di Zhou et al. [29] investigated the effect of tooth profile modification on the dynamic characteristics, which can contribute to improving the dynamic performance of the spur gear system. Hardial Singh et al. [30] proved that Increasing the root radius can significantly improve the performance of helical gears by ensuring more gradual load transfer, thereby reducing shocks and lowering vibration and noise levels. However, the effect of geometric factors, especially the fillet radius, on the nonlinear mesh damping model of gear systems has not been extensively explored. The central idea of the proposed approach is to recast the library design for SINDy to incorporate time-varying stiffness effect. The parameterized library is composed of basis functions whose parameters can be adjusted. Therefore, The main contributions and novel aspects of this work can be summarized as follows:

1) Despite the capability of classical SINDy formulations to handle non-autonomous systems by means of adding time-dependent elements within the library of candidate functions, its utilization on gear systems, with physically characterized time-varying mesh stiffness, is still limited. In this study, the mesh stiffness has been included through a harmonic Fourier series representation within the SINDy library. This way, while estimating damping elements, the effect of changing stiffness due to gear engagement is also considered.

2) This work presents an extended identification strategy for evaluating both linear and nonlinear damping coefficients in spur gear transmissions. The proposed formulation incorporates time-varying stiffness effects within the SINDy framework, enabling the simultaneous estimation of dynamic parameters.

3) Different gear geometries characterized by various fillet radii are considered to study the influence of tooth-root modifications on the identified coefficients. The analysis demonstrates that the nonlinear damping parameters are strongly affected by defect modeling assumptions and radial clearance values.

The remainder of this paper is organized as follows. Section 2 describes the proposed identification methodology, Section 3 details its implementation for spur gear systems, and Section 4 examines the impact of fillet radius variations on the estimated damping coefficients.

2. Identification of nonlinear damping in systems with time-varying stiffness

Among recent extensions of the SINDy framework, SINDy-PI has demonstrated strong capabilities for identifying implicit nonlinear dynamics [10]. Similar to other non-autonomous SINDy formulations, such approaches may accommodate time-dependent terms when appropriately incorporated into the candidate-function library. The contribution of the present work is therefore not based on the general treatment of time-varying systems itself, but rather on the explicit harmonic representation of gear mesh stiffness and its integration into the damping-identification process for gear systems with variable stiffness and fillet-radius effects.

2.1. Sparse identification of nonlinear dynamics approach with time varying stiffness

The basic idea of classical SINDy is first outlined, followed by a modification of the framework to consider variable stiffness. The dynamic behavior of the multi-degree-of-freedom system with time varying stiffness is governed by the nonlinear equation of motion:

$$M\ddot{x}(t) + C_b\,\dot{\mathrm{x}}(\mathrm{t}) + F_{nl} + \left(K_b + \mathrm{K}(\mathrm{t})\right)\mathrm{x}(\mathrm{t}) = \mathrm{f}(\mathrm{t}) \tag{1}$$

where x(t)∈Rn is the generalized displacement vector. K b and C b are respectively the structural stiffness and damping. The stiffness K(t) is time-varying and modeled using a truncated Fourier series, leading to a non-autonomous system. A nonlinear damping that depends on the displacement is defined based on the relative motion between two interacting degrees of freedom i and j:

$$f_{\mathrm{cnl}} = \left(c_{\mathrm{nl0}} + c_{\mathrm{nl2}} x^2\right)\dot{x} \tag{2}$$

The proposed approach aims to estimate both the linear and nonlinear damping coefficients $c_{nl0}, c_{nl1} \ldots . c_{nlM}$.

Although non-autonomous extensions of SINDy allow the inclusion of time-dependent terms or external forcing within the candidate-function library, these formulations generally employ generic temporal dependencies. In the present work, the time-varying stiffness is represented through a physics-based harmonic formulation derived from the periodic gear meshing mechanism. This Fourier-based stiffness representation is incorporated directly into the SINDy library to identify damping coefficients under variable-stiffness conditions and to evaluate the influence of fillet-radius variations on the identified nonlinear damping model. The time varying stiffness K(t) presented in Fig.1 given by the following equation [6]

$$K(t) = K_0 + \sum_{h=1}^{Nh} \left(K_h^{\,c} \cos(\mathrm{hw_m t}) + K_h^{\,s} \sin(\mathrm{hw_m t})\right) \tag{3}$$

Where $K_h^{\,c}$ and $K_h^{\,s}$ are the harmonic coefficients of the time varying stiffness. Nh is the number of harmonic sideband and w m is the mesh frequency.

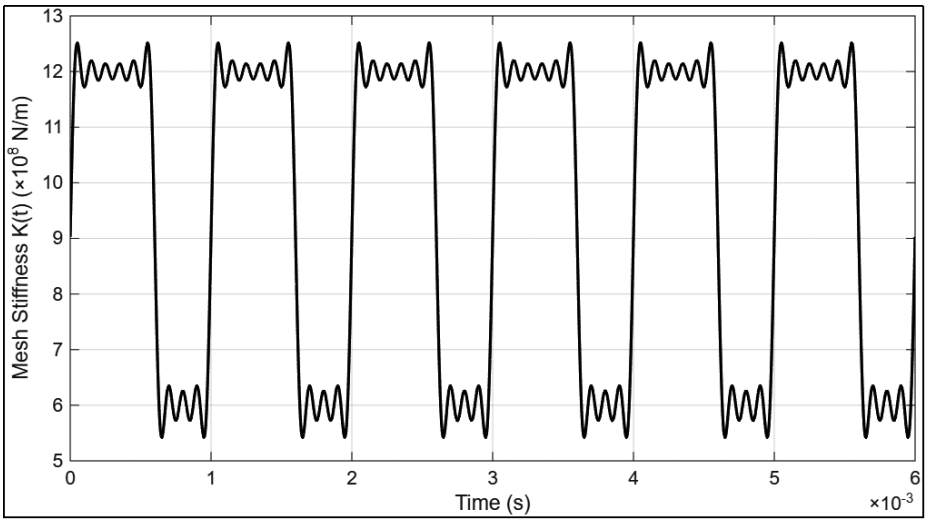


Figure1. Time Varying stiffness

The system is discretized in time into $N_t = 5000$ steps t_k with k = 1, 2,...,N_t. This formulation enables the identification process to account for stiffness evolution. so that all quantities including displacements, velocities, accelerations and the time-varying stiffness are indexed by the discrete time step k. This discretization allows the SINDy regression to capture the time varying conditions at each time step accurately.

After discretization, the dynamic behavior of the multi-degree-of-freedom system is governed by the nonlinear equation of motion:

$$M\ddot{x}_k(t) + C_b\,\dot{\mathrm{x}}_{\mathrm{k}}(\mathrm{t}) + F_{nlk} + \left(K_b + \mathrm{K_k(t)}\right)\mathrm{x_k(t)} = \mathrm{f_k(t)} \tag{4}$$

After discretization, xk = x(tk) denotes the state vector at time step t k. The dynamic equations were integrated using an explicit Forward Euler scheme with a time step of $dt = 5\times10^{-6}$ s over a total simulation duration of 0.02 s. Although explicit

Euler schemes may exhibit stability limitations for highly stiff systems, the adopted time step was selected sufficiently small to ensure stable numerical integration in the present validation example. Convergence was assessed through time-step refinement, and no significant variations were observed in the identified damping parameters. The objective of this numerical example is to validate the proposed identification methodology under controlled time-varying stiffness conditions, while more advanced integration schemes may be considered for strongly stiff industrial gear simulations. In classical SINDy approaches, the library matrix Θ typically includes a large set of generic candidate functions, $1, x, x^2, x^3, x, x\dot{x}, ...$ to capture all possible nonlinearities. However, such a large library increases dimensionality and may include terms with little physical relevance.

In the proposed SINDy method, the library Θ is deliberately minimal and physics-informed:

$$\Theta = \begin{bmatrix} \dot{x}_1 & \dot{x}_1 x^2{}_1 \\ \vdots & \vdots \\ \dot{x}_{Nt} & \dot{x}_{Nt} x^2{}_{Nt} \end{bmatrix} \tag{5}$$

The Challenges in the SINDy technique is presented in the following paragraph. Unlike classical SINDy approaches, the time-varying stiffness K(t) is explicitly included in the target vector:

$$Y_k = -\frac{1}{2}\left[\left(M\ddot{x}_k + K_k x_k - f_k \right)_i - \left(M\ddot{x}_k + K_k x_k - f_k \right)_j \right] \tag{6}$$

This formulation highlights that the identification is performed on a non-autonomous system, where the dynamics depend explicitly on time through K_k. The nonlinear coefficients are identified by solving the regression problem using a regularized least-squares approach.

The solution is given by:

$$\left(\Theta^T \Theta + \lambda I \right)^{-1} \Theta^T Y = \begin{bmatrix} c_{\mathrm{nl}0} \\ c_{\mathrm{nl}2} \end{bmatrix} = \Xi \tag{7}$$

Were $Y = \begin{bmatrix} Y_1 \\ \\ \\ Y_{Nt} \end{bmatrix}$ where λ is a small regularization parameter introduced to improve numerical stability.

This formulation highlights that the identification is performed on a non-autonomous system, where the dynamics depend explicitly on time through K(t). The unknown coefficients are then obtained via ridge regression to improve robustness. Instead of ordinary least squares, ridge regression solves the following equation:

$$\Xi = \arg\min_{\Xi} \left\| \dot{X} - \Theta(X)\Xi \right\| + \lambda \left\| \Xi \right\| \tag{8}$$

Were X is the data matrix of the system states collected over time presented by the following equation:

$$X = \begin{bmatrix} x_1(t_1) & x_2(t_1) & \cdots & x_n(t_1) \\ x_1(t_2) & x_2(t_2) & \cdots & x_n(t_2) \\ \vdots & \vdots & \ddots & \vdots \\ x_1(t_m) & x_2(t_m) & \cdots & x_n(t_m) \end{bmatrix} \tag{9}$$

2.2. Numerical example

To assess the performance of the proposed methodology, a dynamic system characterized by a time-dependent stiffness K(t), a mass matrix M, and a linear damping matrix Clin is considered, as expressed by

$$M = \begin{bmatrix} 2 & & \\ & 5 & \\ & & 3 \end{bmatrix}, K = 10^4 \begin{bmatrix} 5 & 3 & 0 \\ 3 & 5 & 2 \\ 0 & 2 & 1 \end{bmatrix}, C_{\text{lin}} = \begin{bmatrix} 2.25 & 0 & 0 \\ 0 & 3 & 0 \\ 0 & 0 & 0.837 \end{bmatrix} \tag{10}$$

$$f_{\text{c,nl}} = g(c_{\text{nl0}} + c_{\text{nl2}} x^2)\dot{x}, c_{\text{nl0}} = 165, c_{\text{nl2}} = 1.28e4$$

It should be clarified that, in this numerical example, nonlinear damping is present in all three DOFs. Therefore, the identified damping matrix represents the combined contribution of linear and nonlinear effects rather than a purely linear damping component. The SINDy library used in this work is constructed from both linear and nonlinear basis functions. It first includes the velocity terms to capture linear damping effects:

$$\Theta_1 = \dot{q} \tag{11}$$

In addition, nonlinear cubic coupling terms are introduced to represent amplitude-dependent damping behavior:

$$\Theta_2 = q_i q_j^{\,2} \qquad for\, i, j = 1, ..., n \tag{12}$$

Thus, the complete library can be written as:

$$\Theta(q, q) = \left[\dot{q}, q_i q_j^{\,2} \right] \qquad for\, i, j = 1, ..., n \tag{13}$$

The proposed SINDy library is constructed using physically motivated basis functions associated with distinct damping mechanisms. Linear damping contributions are represented through velocity-dependent terms $\dot{q}$, whereas nonlinear damping effects are represented through amplitude-dependent terms involving $\dot{q}q^2$. Since these terms possess different functional structures, the regression procedure can estimate their coefficients independently, allowing separate identification of linear and nonlinear damping contributions without imposing additional external constraints.

This formulation enables the simultaneous identification of linear viscous damping and nonlinear cubic damping contributions within the system dynamics, while maintaining a compact and physically interpretable representation. The simulations were performed using a fixed time step of $\Delta t \approx 5 \times 10^{-6}$ s over a total duration of 0.02 s, corresponding to 4000 temporal samples, and integrated using the forward Euler scheme. In order to further assess the robustness and reliability of the proposed identification framework, a detailed analysis of the obtained results is carried out by comparing the identified coefficients with the reference values used in the numerical simulation. The above comparison shows that the SINDy framework is able to properly model both the linear and nonlinear viscosities present in the system. It is evident from this that the selected basis function library, which is purposely made small for simplicity purposes, still contains the required basis functions to explain the dynamics of the system. **Figure 2** presents the identified damping coefficients. We would like to clarify that the proposed identification framework does not estimate the nonlinear linear coefficient cnl0 independently from the structural linear damping matrix Clin. Instead, the regression identifies the equivalent damping contribution appearing in the governing equations, namely the combined term Clin+cnl0, as shown in Fig. 2(a). From **Figure 2**, the identified equivalent damping matrix Clin+cnl0 is first extracted, and the nonlinear damping coefficient cnl0 is subsequently obtained by subtracting the known structural damping matrix Clin defined in Eq. (10). The resulting identified

values are approximately cnl0 = 165 and cnl2 = 1.28×e4 for the three DOFs, where nonlinear damping is present in all three degrees of freedom. The identified coefficients show excellent agreement with the reference nonlinear coefficients, with negligible discrepancy, thereby indicating a very high identification accuracy.

A quantitative comparison between the reference and identified coefficients presented in **Table 1** confirms the high accuracy of the proposed method. The relative error remains negligible for both cnl0 and cnl2, demonstrating excellent agreement with the reference nonlinear coefficients and supporting the robustness of the identification framework. The sparsity-inducing property of the SINDy identification algorithm, in turn, allows retaining in the resulting equation only those nonlinear terms, which are essential, thus preventing overfitting and increasing the interpretability of the results obtained. At the same time, the nonlinear coefficients identified with this approach match the dynamics of exact values, which proves that amplitude-dependent effects are well-identified and the proposed methodology allows discerning linear and nonlinear dissipation mechanisms from each other. In addition, the presence of time-varying stiffness in the identification does not adversely affect the accuracy of the damping force estimate and even increases the physical accuracy of the identified equation since the parametric excitation effect is taken into account. Moreover, the analysis has shown that in the course of modeling with the proposed approach, stability is guaranteed over the whole-time interval considered, with no substantial difference in the responses of the reference and identified models. These results prove the validity and efficiency of the combination of forward Euler discretization and ridge regression approach applied to non-autonomous systems.

Table 1. Identified damping coefficients and corresponding relative error

Coefficient	Reference coefficients	Identified coefficients	Relative error (%)
cnl0	**165**	**165**	**0**
cnl2	**1.28e4**	**1.28e4**	**0**

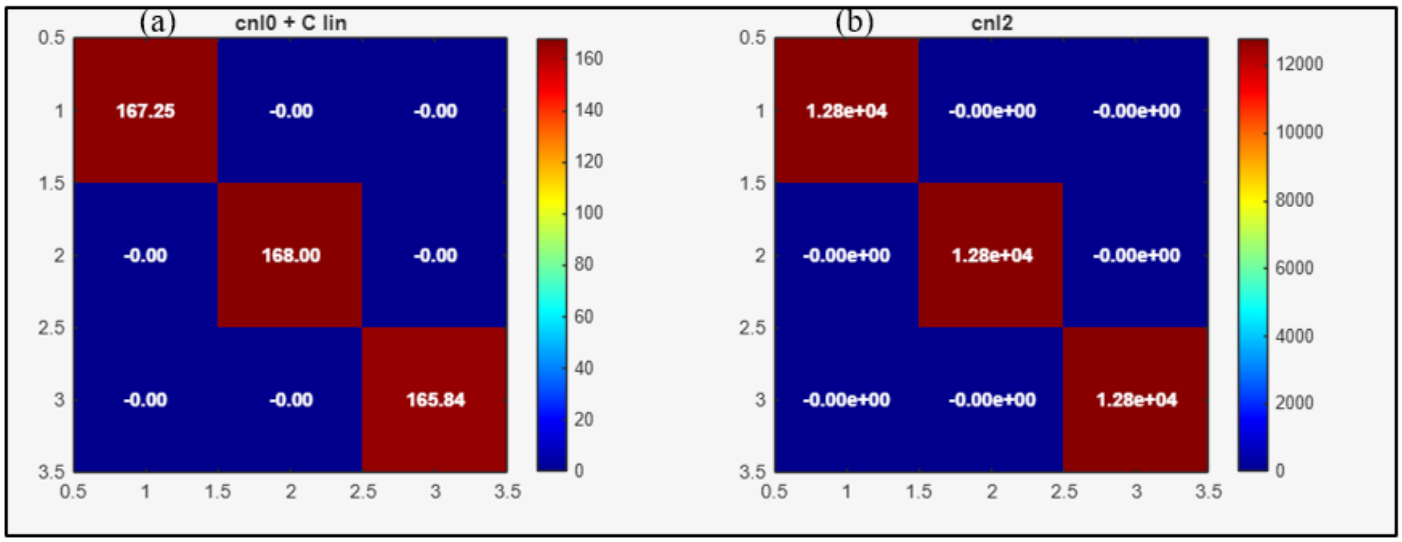


Figure 2. Identified linear and non-linear damping coefficients

After validation on a simple numerical example, the proposed SINDy-based method is further applied to a gear dynamic system. This application aims to demonstrate its capability in identifying both linear and nonlinear damping effects under more realistic operating conditions, including time-varying mesh stiffness and the influence of the filtering ratio Rf.

3. Nonlinear damping estimation in spur gear pairs based on the SINDy method

The SINDy framework introduced in Section 2 is employed to investigate the dynamic behavior of the spur gear pair. The proposed methodology is used to estimate the linear structural damping and the nonlinear damping generated by the interaction between the pinion and the gear.

3.1. Dynamic model of the spur gear pair

The dynamic representation of the spur gear transmission is illustrated in **Figure 3**. The model consists of a pinion, a gear, and a driving motor. The interaction between the pinion and the motor is described by the torsional stiffness k1 and torsional damping coefficient c1, whereas k2 and c2 characterize the coupling between the gear and the external load. The parameters kx1, ky1, cx1, and cy1 denote the equivalent support stiffness and damping coefficients associated with the pinion, while kx2, ky2, cx2, and cy2 correspond to those of the gear. The damping coefficients cx1, cy1, cx2 and cy2 are omitted from **Figure 3** for clarity. The quantities R1 and R2 represent the base circle radii of the pinion and gear, respectively. The mesh damping force adopted in this work is expressed as a quadratic nonlinear damping function given by

$$f_{cnl} = \left(c_{nl0} + c_{nl2}x^2\right)\dot{x} \tag{14}$$

$$where \quad c_{nl0} = 1.32e4 \quad and \quad c_{nl2} = 1.65e5$$

Nonlinear damping in gear systems has been shown to depend on contact and tribological conditions rather than remaining strictly constant [31]. Therefore, the adopted quadratic amplitude-dependent viscous damping model is introduced as a phenomenological approximation capable of representing amplitude-related dissipation while maintaining a compact and interpretable identification framework.

The angular coordinates $\theta m, \theta_1, \theta_1, \theta_L$ denote the rotational motions of the motor, pinion, gear, and load, respectively. The translational displacements of the pinion and the gear along the x and y directions are represented by $x_1, y_1, \mathrm{x}_2, y_2$. Consequently, the mechanical model possesses eight degrees of freedom. The governing dynamic equations of the spur gear system can therefore be written as

$$M\ddot{x}(t) + \left(\mathrm{C} + \mathrm{C_b}\right)\dot{\mathrm{x}}(\mathrm{t}) + \left(Kb + \mathrm{K(t)}\right)\mathrm{x(t)} = \mathrm{f(t)} \tag{15}$$

Where x(t) represents the displacement vector expressed as

$$x(t) = \left[x_1, y_1, \theta m, \theta_1, \theta_2, \theta_L, \mathrm{x}_2, y_2\right] \tag{16}$$

The vector f(t) represents the external excitation acting on the system, while M denotes the mass matrix and Cb corresponds to the structural damping matrix. The interaction between the pinion and the gear is described through a mesh stiffness composed of a constant component Kb and a time-dependent component K(t), such that K = Kb+K(t). The variable stiffness function K(t), previously introduced in Section 2 and defined by Eq. (14), is expressed as follows:

$$K(t) = K_0 + \sum_{h=1}^{Nh} \left(K_h{}^c \cos(\mathrm{hw_m t}) + K_h{}^s \sin(\mathrm{hw_m t})\right) \tag{17}$$

To account for energy dissipation at the gear mesh, a nonlinear damping component is incorporated at the pinion–gear interface. The damping parameters, including both linear and nonlinear contributions, are collected in the vector defined below:

$$u_{lin+nl} = \left[\frac{c_{x1} + c_{y1}}{2}, \frac{c_{x2} + c_{y2}}{2}, c_{c1}, c_{nl0}, c_{c2}, c_{nl1}, c_{nl2} \right] \tag{18}$$

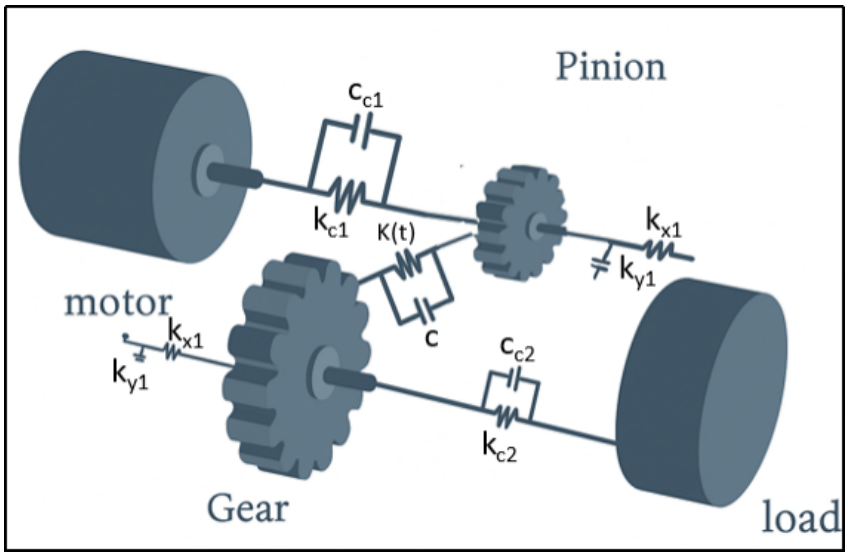


Figure 3. Spur gear pair system

3.2. SINDy algorithm with library optimization for Nonlinear Damping identification

In this work, the nonlinear damping force is identified using a SINDy-inspired regression framework built on physically motivated basis functions. The nonlinear interaction is defined in terms of the relative displacement and relative velocity between the gear pair:

$$\begin{gathered} x_r = q_4 - q_5, \dot{x}_r = \dot{q}_4 - \dot{q}_5 \\ where \quad q_4 = R_1\theta_1, \quad q_5 = R_2\theta_2 \end{gathered} \tag{19}$$

Therefore, the nonlinear damping force is modeled as:

$$f_{nl} = c_{nl0}\dot{x}_r + c_{nl2}{x_r}^2\dot{x}_r \tag{20}$$

The SINDy library is constructed using two physically meaningful basis functions: a linear viscous damping and a nonlinear cubic damping term, where xr is the relative displacement between meshing gears.

The identification uses the following set of basis functions:

-Linear damping term

$$\phi_1 = \dot{x}_r \tag{21}$$

-Nonlinear cubic damping term

$$\phi_2 = {x_r}^2\dot{x}_r \tag{22}$$

The force is approximated as a linear combination of basis functions

$$\mathrm{Y}(t) = \Theta(x)\Xi \tag{23}$$

Where

$$\Theta(x) = [\dot{x}_r \quad {x_r}^2\dot{x}_r] \text{ and } \Xi = \begin{bmatrix} c_{nl0} \\ c_{nl1} \end{bmatrix} \tag{24}$$

This formulation allows the identification of both linear and amplitude-dependent nonlinear damping contributions in the gear system dynamics.

4. Influence of Fillet Radius Rf

4.1. Definition of the three scenarios

To investigate the influence of the fillet radius Rf on the nonlinear dynamic behavior and the identified parameters, three distinct modeling scenarios are considered. These scenarios aim to capture different physical mechanisms through which Rf may affect the system response.

In Scenario A, the fillet radius directly affects the time-varying meshing stiffness. The stiffness function is modified as:

$$K^{(A)}{}_{mesh(t)} = K_{mesh}(t)(1+\alpha r_f * R_f) \tag{25}$$

where αrf = 0.5 is a sensitivity coefficient. This formulation assumes that variations in Rf alter the structural stiffness of the gear contact, leading to a proportional scaling of the meshing stiffness. As a result, the parametric excitation induced by the Fourier-based stiffness K(t) is directly influenced by geometric modifications. **Figure 4** illustrates the impact of fillet radius Rf on time-varying meshing stiffness K(t) is shown in Scenario A, where two different values of Rf have been considered; one with fillet radius equal to zero (Rf = 0 mm) and other with an increased fillet radius (Rf = 0.6 mm). When the fillet radius increases, the overall stiffness level rises slightly, as seen by the higher peaks and elevated baseline of the dashed red curve. This indicates that the fillet radius enhances the local structural rigidity at the tooth root, which in turn scales the meshing stiffness.

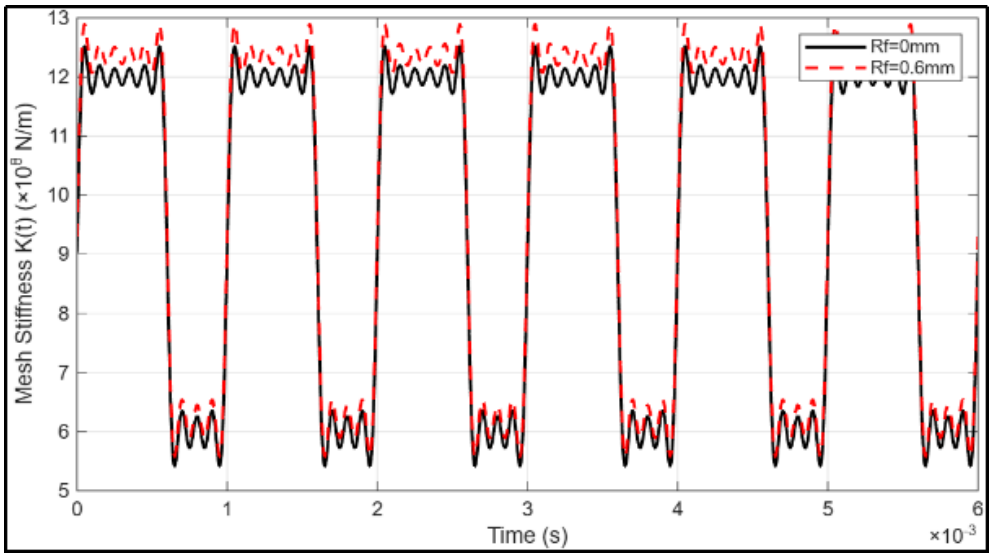


Figure 4. Time varying stiffness for different fillet radii

In Scenario B, the fillet radius influences the nonlinear contact law itself, rather than the stiffness. The nonlinear coefficients are modified as:

$$c_{nl0}{}^{B} = c_{nl0}(1+\beta_{rf} * R_f); c_{nl2}{}^{B} = c_{nl2}(1+\gamma_{rf} * R_f) \tag{26}$$

where β_{rf} = 0.3 and γ_{rf} = 0.3 are sensitivity parameters. This approach reflects the assumption that changes in Rf affect the local contact conditions, such as damping and nonlinear deformation, leading to variations in both linear and nonlinear dissipative effects. It should be clarified that Scenario B does not assume that the

fillet radius directly modifies the intrinsic material damping properties. Instead, the proposed formulation represents an effective contact-level modification induced by geometric changes associated with the fillet radius. Variations in (Rf) may alter the local tooth-root compliance, contact pressure distribution, load-sharing conditions, and microslip behavior during meshing. These effects can indirectly influence the equivalent nonlinear dissipative response identified at the system level. Therefore, the nonlinear coefficients are perturbed to model geometry-induced changes in effective contact behavior rather than intrinsic material damping itself. In Scenario C, the effect of Rf is modeled as a geometric offset in the contact deformation, introducing a shift in the relative displacement:

$$x_k^{\ C} = q_{i,k} - q_{j,k} + \delta_{rf} \tag{27}$$

where $\delta_{rf} = 0.8$ represents a geometry-induced displacement offset. This formulation captures the idea that the fillet radius modifies the initial contact geometry as it presented in **Figure 5**, thereby altering the effective deformation and the nonlinear force response without directly modifying stiffness or coefficients. The three investigated scenarios should therefore be interpreted as complementary parametric sensitivity configurations intended to isolate different mechanisms through which fillet-radius variations may influence the identified nonlinear dynamics, rather than mutually exclusive physical phenomena.

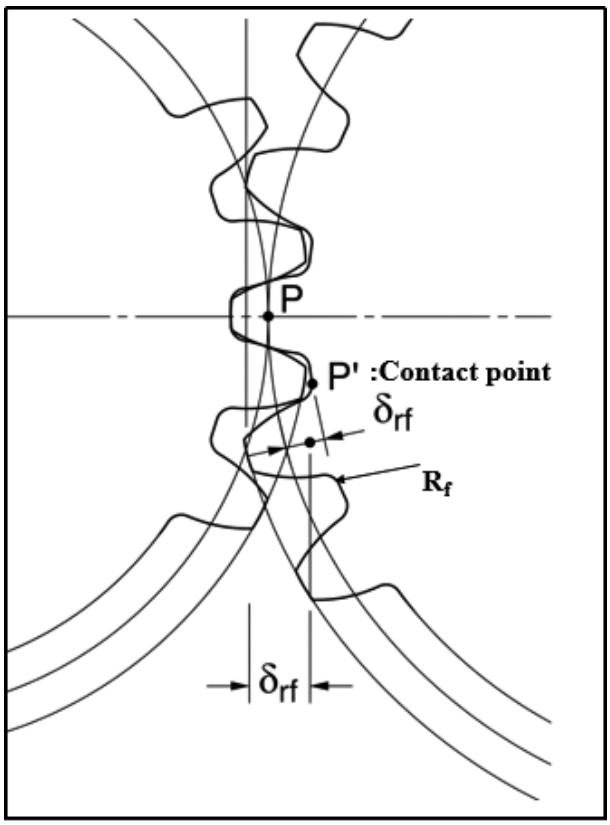


Figure 5. Geometric offset in the contact deformation

All three examples discussed above represent complimentary views on the impact of the fillet radius, namely (i) change of the global stiffness (Example A), (ii) change of intrinsic non-linear characteristics of the contact (Example B), and (iii) geometrical displacement of the contact (Example C). The multi-example approach enables a thorough investigation of the interplay between geometry-related changes and the resulting dynamics of the systems and the

identified nonlinear characteristics. Aside from the independent interpretation of each example, the combination of all three examples reveals additional information about the impact of geometry on the nonlinear system identification process. By considering different aspects of the impact of fillet radius in different examples, one may determine whether any differences in the identified damping coefficients are related to the stiffness changes, intrinsic nonlinearity, or geometry of the contact alone. The discussed scenarios (A, B, and C) are considered as parametric models designed to test the sensitivity of the proposed damping-identification approach to variations in mesh stiffness induced by changes in the fillet radius. In this sense, they cannot be interpreted as mutually exclusive physical phenomena but should be rather viewed as different scenarios of sensitivity analysis. In actual gear assemblies, several effects related to geometry and contact may coexist and affect the behavior of the stiffness/damping mechanism simultaneously; the proposed framework may accommodate these simultaneous effects via incorporating them into the candidate function library.

In other words, these models do not describe completely arbitrary phenomena but rely on some measurable fillet radius variations that are considered in engineering practice. The main motivation behind introducing these scenarios relies on previous studies indicating the effect of the fillet radius on stiffness variation and overall gear dynamics. It is aimed at providing a basis for discussing the sensitivity trends prior to performing a detailed validation using geometry-based or FEM models. Previous studies [26-30] confirmed that the fillet radius affects tooth root stresses, stiffness evolution, and gear dynamics.

4.2. Impact of Fillet Radius Rf on the nonlinear damping coefficients

This section presents the effect of fillet radius on linear and nonlinear damping coefficients in the case of the three scenarios with Rf = 1mm. **Figure 6** presents the identified linear damping matrices, the damping values obtained using the SINDy method correspond closely to the reference values , confirming the accuracy of the proposed identification strategy for linear dissipation. A quantitative comparison between the reference and identified coefficients presented in **Table 2** shows that the identification procedure accurately estimates the linear nonlinear damping coefficient cnl0, with a negligible relative error close to 0. This indicates that the lower-order damping term is robust and weakly affected by modeling uncertainties.

In contrast, the higher-order nonlinear coefficient cnl2 exhibits larger variations depending on the considered case. Scenario C provides the most accurate estimation, with a relative error of only 0.78%, whereas Scenario A and Scenario B lead to higher deviations of 3.13% and 23.44%, respectively.

These results indicate that the coefficient cnl2 is significantly more sensitive than cnl0 to modeling assumptions and parameter perturbations. This behavior is physically expected because the nonlinear damping contribution depends on the higher-order term which amplifies small variations in displacement and velocity during the identification process. Overall, the results confirm that the proposed identification framework reliably captures the dominant nonlinear damping behavior, while higher-order coefficients remain inherently more sensitive to uncertainties and noise.

Table 2. Identified damping coefficients and corresponding relative errors

Coefficient	Reference coefficients	Identified coefficients	Relative error (%)
cnl0	**132**	**132**	**0**
		Scenario A : 1.24e4	**3.13**
cnl2	**1.65^{e}5**	**Scenario B : 1.58e4**	**23.44**
		Scenario C : 1.29e4	**0.78**

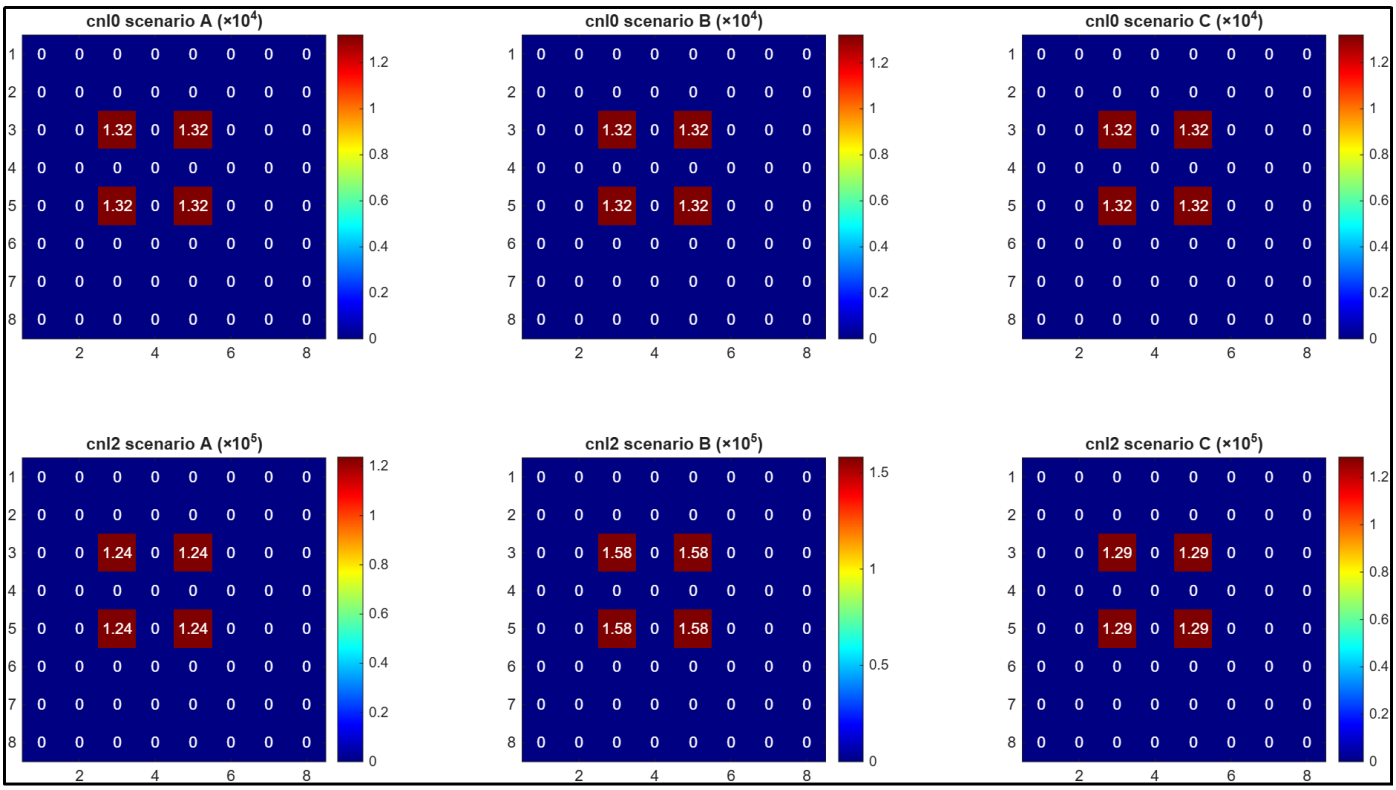


Figure 6. Identified linear and non-linear damping coefficients in the case as of three scenarios

4.3. Damping identification with varying fillet radius Rf

In order to explore the effect of fillet radius on damping identification, new simulations have been performed for two cases corresponding to Rf = 0.6 mm and Rf = 0.8 mm. Contrary to the reference case with Rf = 1 mm shown in Fig. 6, the findings reported in this part and shown in **Figure 7** refer to a parametric study that intends to explore the sensitivity of the identified damping coefficients to changes in fillet radius. The considered fillet radii (Rf = 0.6 mm and Rf = 0.8 mm) were chosen to be characteristic of geometric variations close to those considered previously in spur gears [26] where fillet radii like 0.5 mm, 0.76 mm (nominal) and 1.0 mm were studied. In this paper, attention is drawn to relatively small changes about the reference case (Rf = 1 mm). In doing so, realistic physical parameters are used. The obtained results, presented in Fig.7, highlight the sensitivity of the identified nonlinear damping parameters under different defect modelling scenarios and radial clearance levels. The linear coefficient cnl0 remains nearly constant across all cases, with values around 1.32e4, indicating that this term is weakly affected by the introduced variations and can be considered structurally robust. In contrast, the nonlinear coefficient cnl2 exhibits significant variations depending on the scenario

and radial clearance. In Scenario A, where the defect is applied through stiffness modification, a noticeable reduction in cnl2 is observed as the radial clearance increases, suggesting a redistribution of nonlinear contact effects. Scenario B, where the nonlinear parameters are directly perturbed, leads to a moderate increase in cnl2, reflecting the imposed parameter sensitivity. Finally, Scenario C, which introduces a contact displacement shift, produces the most pronounced amplification of cnl2, reaching the highest values among all cases. This indicates that geometric misalignment or contact pre-displacement strongly enhances nonlinear interactions within the system. The displacement shift alters the effective contact kinematics and consequently changes the nonlinear deformation response during meshing. Since cnl2 represents the amplitude-dependent damping contribution, it becomes more sensitive to this geometric perturbation than the linear damping component cnl0. Therefore, the stronger amplification of cnl2 observed in Scenario C is interpreted as a consequence of the altered contact deformation mechanism induced by the geometric offset.

Overall, it can be seen that the dynamics are controlled mainly through contact conditions rather than linear damping properties, with cnl2 being an important measure for indicating the impact of contact nonlinearities. From the analysis performed, there are further indications that the nonlinear damping parameter serves as an important and sensitive measure for detecting contact conditions and other geometric imperfections within the gear system. More specifically, the significant variability in the value of cnl2 between various scenarios implies that the effects of nonlinear damping dissipations depend greatly on contact conditions rather than general characteristics of the system. Therefore, the necessity to capture geometric properties, such as the fillet radius, is essential for obtaining good results in parameter identification tasks.

As shown from the results, the nonlinear parameter cnl2 demonstrated significantly greater variations compared to the linear one. This is explained by the fact that nonlinear damping depends greatly on variations in the stiffness and dynamic state of the system. Additionally, as nonlinear terms could be more sensitive to measurement errors, another sensitivity study was carried out using added noise. The results demonstrated that although cnl2 presents higher sensitivity than cnl0, the proposed identification framework preserves stable and physically meaningful damping trends under moderate noise conditions. Additionally, the differences observed between the two fillet radius values (0.6 mm and 0.8 mm) confirm that even small geometric modifications can lead to noticeable changes in the identified nonlinear response. This sensitivity underscores the limitations of simplified models that neglect such parameters, especially in high-precision applications. From a methodological perspective, the ability of the proposed SINDy framework to capture these variations demonstrates its effectiveness in detecting subtle nonlinear effects embedded in the system dynamics.

Moreover, the results suggest that Scenario C may represent the most critical case for practical applications, as it captures geometric misalignment effects that are commonly encountered in real gear systems. Consequently, incorporating such geometric considerations into data-driven identification approaches is essential for improving both predictive accuracy and physical relevance.

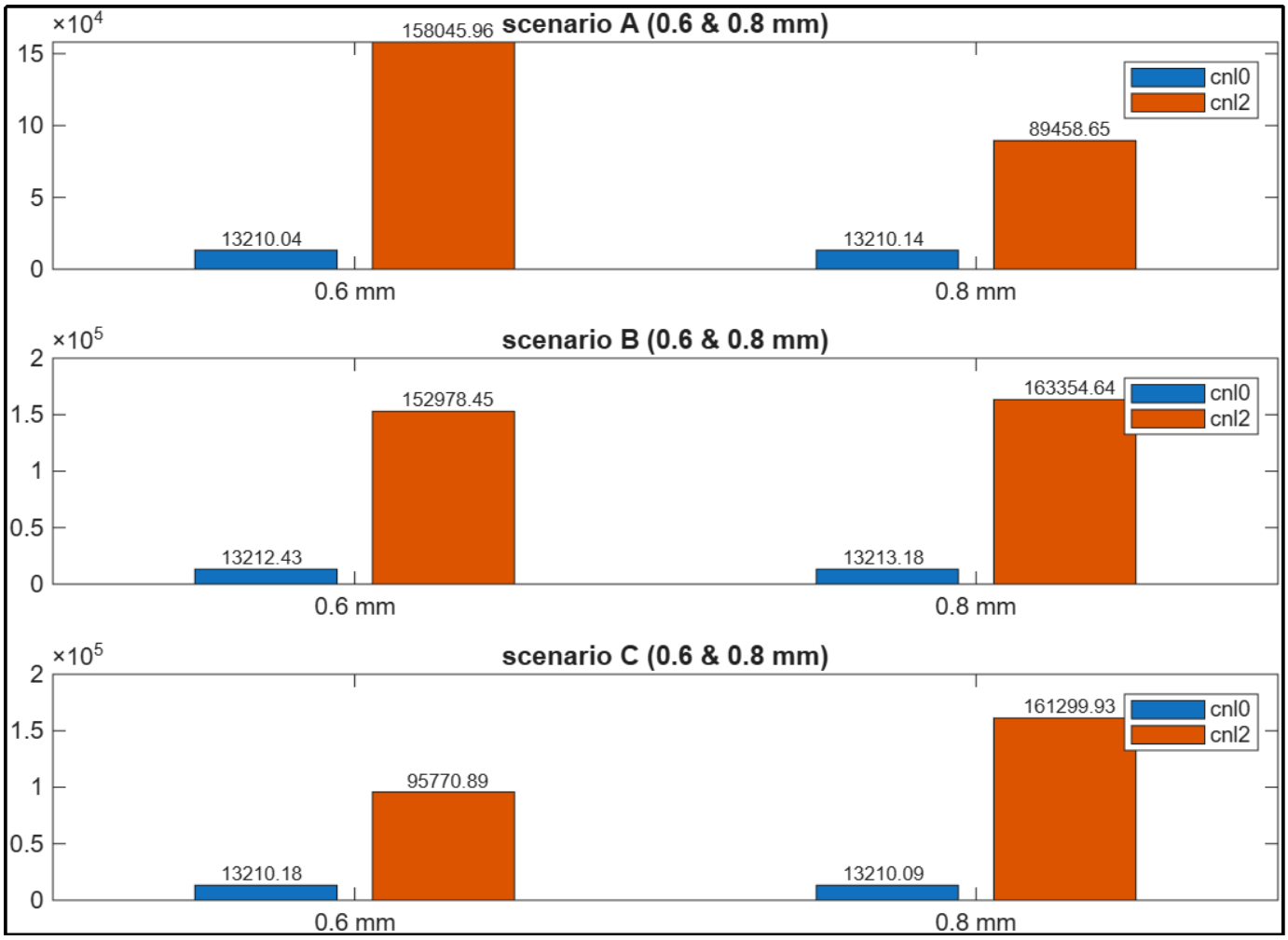


Figure 7. Effect of fillet radius modification on the linear and non-linear damping coefficients

4.4. Robustness assessment under noisy conditions

To evaluate the robustness of the proposed identification procedure, Gaussian measurement noise was added to the simulated displacement and velocity signals. The acceleration signal was intentionally kept noise-free in order to avoid numerical amplification during the regression process.The obtained results presented n **Figure 8** showed that the identified coefficient cnl0 remained relatively stable under noisy conditions, whereas cnl2 exhibited higher sensitivity to measurement perturbations. In the noise-free case, the identified value of cnl2 was approximately 1.29e5, while under noisy conditions it increased to approximately 2.76e5. This behavior is expected because the higher-order nonlinear term depends on which is inherently more sensitive to noise and regression conditioning effects. Nevertheless, the identification framework remained capable of capturing the dominant nonlinear damping behavior, confirming the robustness of the proposed methodology.

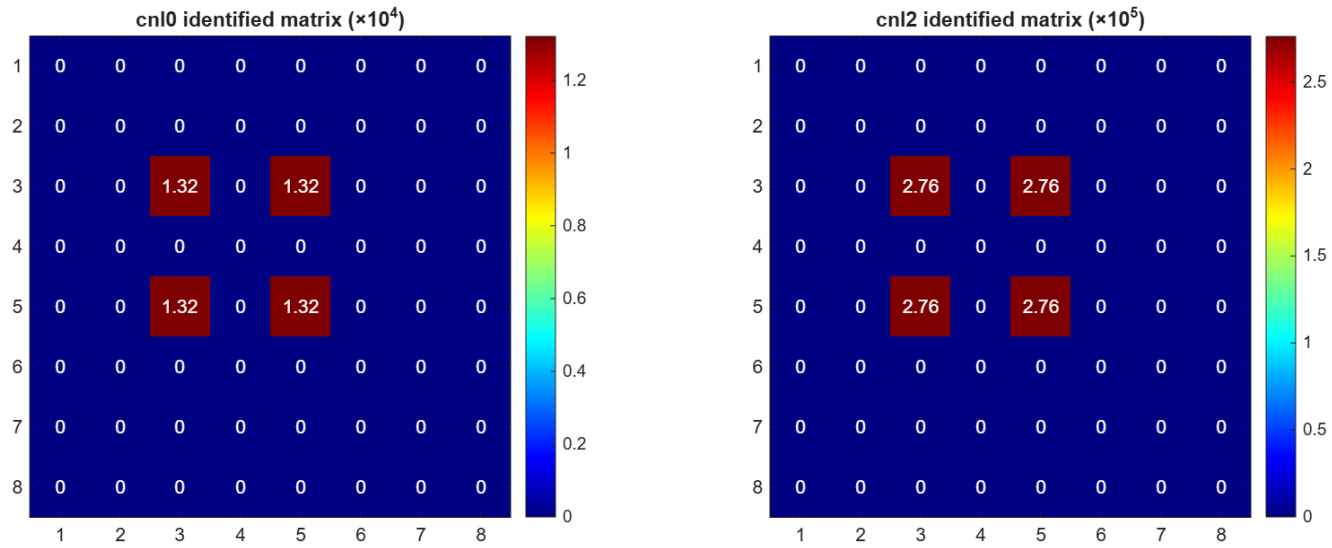


Figure 8. Identified linear and non-linear damping coefficients under noisy conditions

5. Conclusion

In this work, we have suggested an expanded SINDy framework for identifying nonlinear damping in spur gear drives considering their non-linear properties arising from the time-varying stiffness. The proposed framework considers the parameterized library based on a harmonic representation accounting for the variations in stiffness due to time. We performed extensive parametric analysis concerning the influence of fillet radii on the performance of identification for various cases of modelling. It was shown that geometric features, especially the fillet radius, affect both the dynamics of the system and the resulting nonlinear damping terms, emphasizing the necessity to consider such physical characteristics when employing purely data-driven identification tools. This study reveals that geometric features such as fillet radius are not merely secondary design parameters, but play a critical role in the accuracy of data-driven identification methods, thereby opening new perspectives for geometry-informed system identification. In addition to the theoretical contributions, the proposed framework also provides practical insights for the design and analysis of gear systems operating under complex dynamic conditions. By explicitly linking geometric parameters to the identified nonlinear damping behavior, this study offers a pathway toward more accurate predictive models that can be used in condition monitoring, fault detection, and performance optimization. The integration of time-varying stiffness within the SINDy framework further enhances its applicability to real-world systems, where operating conditions are rarely stationary and often influenced by periodic excitations. Furthermore, the proposed methodology can be extended to other classes of mechanical systems exhibiting strong nonlinearities and parameter variations, making it a versatile tool for data-driven system identification. The use of a physics-informed and reduced-order library ensures a balance between model simplicity and descriptive capability, which is essential for both computational efficiency and interpretability. Although the proposed framework demonstrated accurate and robust nonlinear damping identification under time-varying stiffness conditions, the present study remains limited to numerical simulations and simplified parametric representations of fillet-radius effects. The investigated scenarios were intended as physically motivated sensitivity configurations and were not validated using detailed finite-element contact analysis or experimental measurements.

From an engineering perspective, the findings highlight the importance of

incorporating geometric design parameters into identification procedures, particularly when high fidelity models are required. Future work may focus not only on experimental validation but also on the integration of uncertainty quantification and noise robustness, as well as the extension of the framework to more complex gear configurations and multi-stage transmission systems.

To summarize, our paper presents a novel framework for constructing the library used in SINDy for a wide class of nonlinear systems whose parameters can vary along the time axis. Future directions could be related to validating the suggested method experimentally.

Author contributions: NY, FM and AA: original draft preparation, visualization, validation and investigation; LW: methodology and software, contributed to the discussions and first reviewing; MH: supervision, reviewing and editing. All authors have read and agreed to the published version of the manuscript.

Funding: None.

Acknowledgment: None.

Conflict of interest: The authors declare no conflict of interest.

Data availability statement: The data used to support the findings of this study are available from the corresponding author upon request

AI use statement: The authors confirm that the manuscript was written by themselves. AI-based tools were used only for minor language polishing and grammar suggestions and did not contribute to the scientific content, analysis, or interpretation of the work.

References

1. P. Balasubramanian, G. Ferrari, M. Amabili, Identification of the viscoelastic response and nonlinear damping of a rubber plate in nonlinear vibration regime, Mech. Syst. Signal Process. 111, 376–398, 2018. doi: 10.1016/j.ymssp.2018.03.061.
2. Zhang, L., Qu, D., Jiang, H. et al. Dynamic analysis of gear systems with dynamic mesh stiffness and time-varying bearing stiffness. Nonlinear Dyn 113, 28883–28906 (2025). doi: 10.1007/s11071-025-11653-8.
3. Safari, S.; Londoño Monsalve, J.M. Data-driven structural identification of nonlinear assemblies: Asymmetric stiffness and damping nonlinearities. Mechanical Systems and Signal Processing, 222, 111745, 2025. doi: 10.1016/j.ymssp.2024.111745.
4. Safari, S.; Londoño Monsalve, J.M. Data-driven structural identification of nonlinear assemblies: Uncertainty Quantification. International Journal of Non-Linear Mechanics, 170, 105002, 2025. doi: 10.1016/j.ijnonlinmec.2024.105002.
5. Al-hababi, T., Cao, M., Saleh, B., Alkayem, N. F., & Xu, H. (2020). Critical review of nonlinear damping identification in structural dynamics: Methods, applications, and challenges. Sensors, 20(24), 7303. doi: 10.3390/s20247303.
6. Nourhaine Yousfi, Fatma Mejdoub, Ali Akrout, Lassaad Walha, Mohamed Haddar, Nonlinear damping identification using extended continuous wavelet transform and long-short term memory: Application to a spur gear pair system. S V, Sound and Vibration, 2026, 60(2), 3869. doi: 10.59400/sv3869.
7. Fehr, J., Kargl, A., Eschmann, H.: Identification of friction models for mpc-based control of a powercube serial robot. preprint arXiv:2203.10896 (2022). doi: 10.48550/arXiv.2203.10896.
8. S. L. Brunton, J. L. Proctor, and J. N. Kutz, Discovering governing equations from data by sparse identification of nonlinear dynamical systems, Proceedings of the National Academy of Sciences, vol. 113, pp. 3932–3937, 2016. doi: 10.1073/pnas.1517384113.
9. Didonna, M., Stender, M., Papangelo, A., Fontanela, F., Ciavarella, M., Hoffmann, N.: Reconstruction of governing equations from vibration measurements for geometrically nonlinear systems. Lubricants 7(8), 64 (2019). doi: 10.3390/lubricants7080064.
10. K. Kaheman, J. N. Kutz, and S. L. Brunton, SINDy-PI: a robust algorithm for parallel implicit sparse identification of nonlinear dynamics, Proceedings of the Royal Society A: Mathematical, Physical and Engineering Sciences, vol. 476, p. 20200279, 2020. doi: 10.1098/rspa.2020.0279.

11. E. Kaiser, J. N. Kutz, and S. L. Brunton, "Sparse identification of nonlinear dynamics for model predictive control in the low-data limit," Proceedings of the Royal Society A: Mathematical, Physical and Engineering Sciences, vol. 474, p. 20180335, 2018.
12. R. Cao, Y. Lu, and Z. He, System identification method based on interpretable machine learning for unknown aircraft dynamics, Aerospace Science and Technology, vol. 126, p. 107593, 2022. doi: 10.1016/j.ast.2022.107593.
13. A. Yonezawa, H. Yonezawa, S. Yahagi, I. Kajiwara, S. Kijimoto, H. Taniuchi, and K. Murakami, "Sparse identification of nonlinear dynamics with library optimization mechanism: Recursive long-term prediction perspective," IEEE Trans. Cybern., 2026, pp. 1–14. doi: 10.1109/TCYB.2026.3652850.
14. F. Abdullah and P. D. Christofides, Data-based modeling and control of nonlinear process systems using sparse identification: An overview of recent results, Computers & Chemical Engineering, vol. 174, p. 108247, 2023. doi: 10.1016/j.compchemeng.2023.108247.
15. Lathourakis, C., Cicirello, A. Physics enhanced sparse identification of dynamical systems with discontinuous nonlinearities. Nonlinear Dyn 112, 11237–11264 (2024). doi: 10.1007/s11071-024-09652-2.
16. Zhang L, Schaeffer H. 2019 On the convergence of the SINDy algorithm. Multiscale Model. Simul. 17, 948–972. doi: 10.1137/18M1189828.
17. M. Dam, M. Brøns, J. J. Rasmussen, V. Naulin, and J. S. Hesthaven, Sparse identification of a predator-prey system from simulation data of a convection model, Physics of Plasmas, 24 (2017), 022310.
18. F. Kiarasi, A. Asadi, M. Babaei, K. Asemi, M. Hosseini, Dynamic analysis of functionally graded carbon nanotube (FGCNT) reinforced composite beam resting on viscoelastic foundation subjected to impulsive loading, J. Comput. Appl. Mech., 53(1), 1–23, 2022. doi: 10.22059/JCAMECH.2022.339008.693.
19. Hesam Nazari, Masoud Babaei, Faraz Kiarasi, Kamran Asemi, Geometrically nonlinear dynamic analysis of functionally graded material plate excited by a moving load applying first-order shear deformation theory via generalized differential quadrature method, SN Applied Sciences (2021) 3:847. doi: 10.1007/s42452-021-04825-9.
20. Adam Purnomo & Mitsuhiro Hayashibe, Sparse identification of Lagrangian for nonlinear dynamical systems via proximal gradient method, Scientific Reports (2023) 13:7919. doi: 10.1038/s41598-023-34931-0.
21. Loiseau, J. C. & Brunton, S. L. Constrained sparse Galerkin regression. J. Fluid Mech. 838, 42–67 (2018). doi: 10.48550/arXiv.1611.03271.
22. Yahagi, S., Seto, H., Yonezawa, A. et al. Sparse Identification and Nonlinear Model Predictive Control for Diesel Engine Air Path System. Int. J. Control Autom. Syst. 23, 620–629 (2025). doi: 10.1007/s12555-024-0452-9.
23. K. Champion, P. Zheng, A. Y. Aravkin, S. L. Brunton, and J. N. Kutz, A Unified Sparse Optimization Framework to Learn Parsimonious Physics-Informed Models From Data, IEEE Access, vol. 8, pp. 169259–169271, 2020. doi: 10.48550/arXiv.1906.10612.
24. N. M. Mangan, S. L. Brunton, J. L. Proctor, and J. N. Kutz, Inferring Biological Networks by Sparse Identification of Nonlinear Dynamics, IEEE Trans. Mol. Biol. Multi-Scale Commun., vol. 2, no. 1, pp. 52–63, Jun. 2016. doi: 10.48550/arXiv.1605.08368.
25. Champion, K., Lusch, B., Kutz, J.N., Brunton, S.L., Data-driven discovery of coordinates and governing equations, Proc. Natl. Acad. Sci., 116(45), 22445–22451, 2019. doi: 10.1073/pnas.1906995116.
26. Abderrahim Baccar, Ahmed Samet, Ahmed Hammami, Nuno Dourado, Ali Akrout, Mohamed Haddar, Impact of Fillet Radius on Mesh Stiffness and Performance of Polyoxymethylene (POM) Spur Gears: A Parametric Numerical Study, 2026, Eng. Res. Express, in press. doi: 10.1088/2631-8695/ae59f3.
27. A. W. Hussein and M. Q. Abdullah, 'A Novel Fillet Form for Non-Generation Cutting Gear Teeth', Results in Engineering, vol. 16, p. 100523, Dec. 2022. doi: 10.1016/j.rineng.2022.100523.
28. S. Senthilvelan and R. Gnanamoorthy, 'Effect of gear tooth fillet radius on the performance of injection molded Nylon 6/6 gears', Materials & Design, vol. 27, no. 8, pp. 632–639, Jan. 2006. doi: 10.1016/j.matdes.2004.12.015.
29. Zhou, D.; Guo, Y.; Yang, J.; Zhang, Y. Study on the Parameter Influences of Gear Tooth Profile Modification and Transmission Error Analysis. Machines 2024, 12, 316. doi: 10.3390/machines12050316.
30. Hardial Singh S.B. Gupta. Effect of Fillet Radius on Bending Stress in Helical Gear using FEA, Journal of Polymer & Composites, Volume 11, Special Issue 8, 2023. http://engineeringjournals.stmjournals.in/index.php/JoPC/index.
31. S. Liu and F. Liu, "Vibration characteristics of spur gear system with non-linear damping under no lubrication condition," Journal of Vibroengineering, Vol. 21, No. 5, pp. 1260–1270, Aug. 2019. doi: 10.21595/jve.2019.20248.